Macromolecules
ARTICLE

Macromolecules **2009**, *42*, 9325–9331 **9325**
DOI: 10.1021/ma901651f

New Understanding in Tuning Toughness of β-Polypropylene: The Role of β-Nucleated Crystalline Morphology

Feng Luo,[†] Chengzhen Geng,[†] Ke Wang,*[,†] Hua Deng,[†] Feng Chen,[†] Qiang Fu,*[,†] and Bing Na[‡]

[†]*College of Polymer Science and Engineering, State Key Laboratory of Polymer Materials Engineering, Sichuan University, Chengdu 610065, People's Republic of China, and* [‡]*Department of Materials Science and Engineering, East China Institute of Technology, Fuzhou 344000, People's Republic of China*

Received July 26, 2009; Revised Manuscript Received October 23, 2009

ABSTRACT: It is widely believed that the trigonal β-form is favorable and effective for toughening isotactic polypropylene (iPP). Therefore, β-form content should be achieved as high as possible to realize excellent toughness in iPP. However, in this study, we demonstrate that the connection between crystallites might mainly determine the toughness of iPP instead of the β-crystal content. A new rare earth nucleator (WBG) was used to generate the rich β-crystalline structure in the compression-molded bars that were fabricated upon different molten temperatures (T_f). Interestingly, the increase in tensile elongation can be as large as 8 times for increased T_f. The polymorphic composition and overall crystallinity of β-nucleated iPP are almost independent of T_f. Nevertheless, the β-nucleated crystalline morphology has completely changed. Three types of β-crystalline morphology, namely, β-spherulite, β-transcrystalline entity, and "flower"-like agglomerate of β-crystallites, are sequentially obtained with increasing T_f. From the morphological point of view, the connection between the crystallites in "flower"-like agglomerate is significantly better than that for the crystallites generated under lower T_f. Therefore, it is concluded that the formation of β-nucleated iPP provides very good toughness only with sufficient connection between the crystallites. The result of this study clearly verifies the importance of crystal morphology on tuning the toughness of iPP. It provides important information for potential industrial applications.

1. Introduction

Isotactic polypropylene (iPP) is one of the most important thermoplastic polymers owing to its low manufacturing cost and rather versatile properties. It is a typical polymorphic plastic with at least four basic crystalline forms, namely, the monoclinic α-form, trigonal β-form, orthorhombic γ-form, and mesomorphic smectic form.[1−4] Among these crystalline forms, the β-form usually shows excellent toughness, so it has received much attention from scientific research and industrial applications.[5−10] Compared with the α-form obtained under common processing conditions, β-form may only be generated under some specific conditions, such as quenching,[5] abrupt temperature gradient,[6] shearing or elongation deformation,[7−10] and the addition of β-nucleating agent.[11−23] Among these methods, the addition of β-nucleating agent is the most effective and accessible method to obtain high β-form content in iPP.

In terms of mechanical properties, it has been demonstrated that the presence of β-form crystal leads to enhanced toughness and ductility. In general, excellent toughness is attributed to energy dissipation during yield process accompanied by phase transformation from β to α form.[15] The studies on the deformation mechanism of β-form iPP have indicated that interlamellar slippage[16,17] and crazing development[18,19] were the dominant modes for phase transformation. It is widely accepted that a higher content of β-crystal is desired to achieve higher toughness. Many researchers were devoted to increase β-form content in iPP efficiently. Varga et al.[20] demonstrated that the final temperature of heating, nucleator concentration, and thermal conditions during cooling and crystallization played a very important role in the supermolecular structure of β-nucleated iPP and indicated that various β-crystalline morphologies might exist in iPP. Consequently, it has raised the question for the role of β-crystalline morphology on the macroscopic toughness of β-nucleated iPP. To the best of our knowledge, discussion on this subject is rarely reported in the open literature. The main problem might be that many β nucleators have dual nucleating ability,[20] which enhances both α- and β-form crystals in iPP. Therefore, the polymorphic composition and crystallinity are altered simultaneously with the change of crystalline morphology in most cases. Therefore, it is hard to estimate the individual effect of crystalline morphology among various influential factors.

In this study, a new rare earth β-nucleating agent (designated as WBG), which has been synthesized and investigated by Feng's group,[21,22] was adopted to prepare β-PP. Its composition is heteronuclear dimetal complexes of lanthanum and calcium containing some specific ligands. WBG exhibits very high β-selectivity and efficiency. The compression-molded bars of iPP with a fixed WBG content of 0.25 wt % were prepared under different final molten temperatures (T_f). Thanks to the high β-selectivity and nucleating efficiency of WBG, the polymorphic compositions and crystallinities are almost identical under different T_f values, but the β-crystalline morphologies are quite different for different T_f values. It is then possible to investigate the relationship between inherent crystalline morphology and macroscopic toughness.

2. Experimental Section

2.1. Materials and Sample Preparation. A commercially available isotactic polypropylene (iPP), purchased from Dushanzi Petroleum Chemical Incorporation (Xinjiang, China), with $M_w = 39.9 \times 10^4$ g/mol and $M_w/M_n = 4.6$, was adopted as

*Corresponding author. Tel: 0086-28-85405402. E-mail: qiangfu@scu.edu.cn (Q.F.); wkestar@scu.edu.cn (K.W.).

Published on Web 11/05/2009

basal resin. A small amount of antioxidant (Irganox 1010) has been added to the as-received iPP. The rare earth β-nucleating agent, marked as WBG-II, was kindly supplied by Winner Functional Materials (Foshan, Guangdong, China). The raw WBG is a kind of irregular blocklike crystal. The single crystal diameter is about tens of nanometers, and most of the agglomerates consist of several crystals.

The iPP and WBG powders were first melt compounded to make a master-bath containing 5 wt % WBG in a corotating twin screw extruder; then, the master-bath and pure iPP were extruded to prepare iPP specimens containing 0.25 wt % WBG. The pelletized granules were subsequently compression molded under various final molten temperatures, selected as 180, 200, 220, and 240 °C. The specimens were compressed under a pressure of 5 MPa for 10 min. Then, the specimens were relocated to another press at room temperature to cool down under a pressure of 10 MPa in air. For comparison purpose, the compression-molded bars of neat iPP and α-nucleated iPP (with 0.25 wt % α-nucleator) were also prepared under the same processing procedure mentioned above, and a bis-(3,4-dimethylbenzylidene) sorbitol (DMDBS, Millad 3988, Milliken Chemical) was used as α-nucleator.

2.2. Measurements. Standard tensile tests were performed using an SANS Universal tensile testing machine controlled by a two-step program, according to the GB/T 1040−92 standard. The notched izod impact strength of the specimens was tested with a VJ-40 izod machine according to the GB/T 1834−1996 standard. All mechanical properties were measured under room temperature (about 25 °C), and the average value was obtained from over five specimens for each condition.

A Philips X'Pert pro MPD apparatus was adopted to acquire WAXD spectra. The analysis method of WAXD spectra was described elsewhere by Huo et al.[23] The overall crystallinity, X_c, was calculated according to the following equation

$$X_c = \frac{\sum A_{cryst}}{\sum A_{cryst} + \sum A_{amorp}}$$

where A_{cryst} and A_{amorp} are the fitted areas of crystal and amorphous region, respectively, whereas the relative amount of the β-form crystal, K_β, was evaluated according to the method of Turner-Jones et al.[5] as

$$K_\beta = \frac{A_{\beta(300)}}{A_{\alpha(110)} + A_{\alpha(040)} + A_{\alpha(130)} + A_{\beta(300)}}$$

where $A_{\beta(300)}$ is the area of the (300) reflection peak of β-form at $2\theta = 16.1°$; $A_{\alpha(110)}$, $A_{\alpha(040)}$, and $A_{\alpha(130)}$ are the areas of the (110), (040), and (130) reflection peaks of the α-form and correspond to $2\theta = 14.1$, 16.9, and 18.6°, respectively.

The SEM experiments were performed using a Hitachi S3400+EDX SEM instrument to inspect the cryofractured surface of β-PP etched by a mixed acid solution.[24] The samples were gold-coated and observed under an acceleration voltage of 20 kV. Morphological observations of β-PP crystallite growth were performed on a Leica DMIP polarized light microscopy (PLM) equipped with a Linkam THMS 600 hot stage under crossed polarizer. The extruded β-PP granules were heated to various final molten temperatures and kept for 10 min to achieve the same thermal history as the compression molded samples. Subsequently, the molten films were cooled to room temperature in air. The morphological photographs of crystallization were recorded with the aid of a digital camera during cooling. The rheological measurements were performed in linear viscoelastic regime on a stress-controlled Gemini 200 rheometer (Malvern Instruments, U.K.) using a dynamic temperature sweep mode under an oscillation frequency of 0.1 rad/s. The samples were heated to various final molten temperatures and kept at those temperatures for 5 min. They were then cooled to 130 °C at a rate of 3 °C/min. All rheological measurements were conducted under a nitrogen atmosphere.

3. Results and Discussion

3.1. Mechanical Properties of the Compression-Molded Bars. On the basis of the research goal of this study, the effect of T_f on the mechanical properties in β-nucleated iPP is studied. The stress−strain curves for pure iPP, α-nucleated iPP, and β-nucleated iPP samples prepared upon different T_f values are presented in Figure 1. The stress−strain behaviors for neat iPP and α-nucleated iPP are almost the same for various final molten temperatures. Meanwhile, by comparing α-nucleated iPP with neat iPP, the elongation at break is obviously decreased by additional α-nucleator. For the β-nucleated iPP bars, a notable feature in tensile behavior is

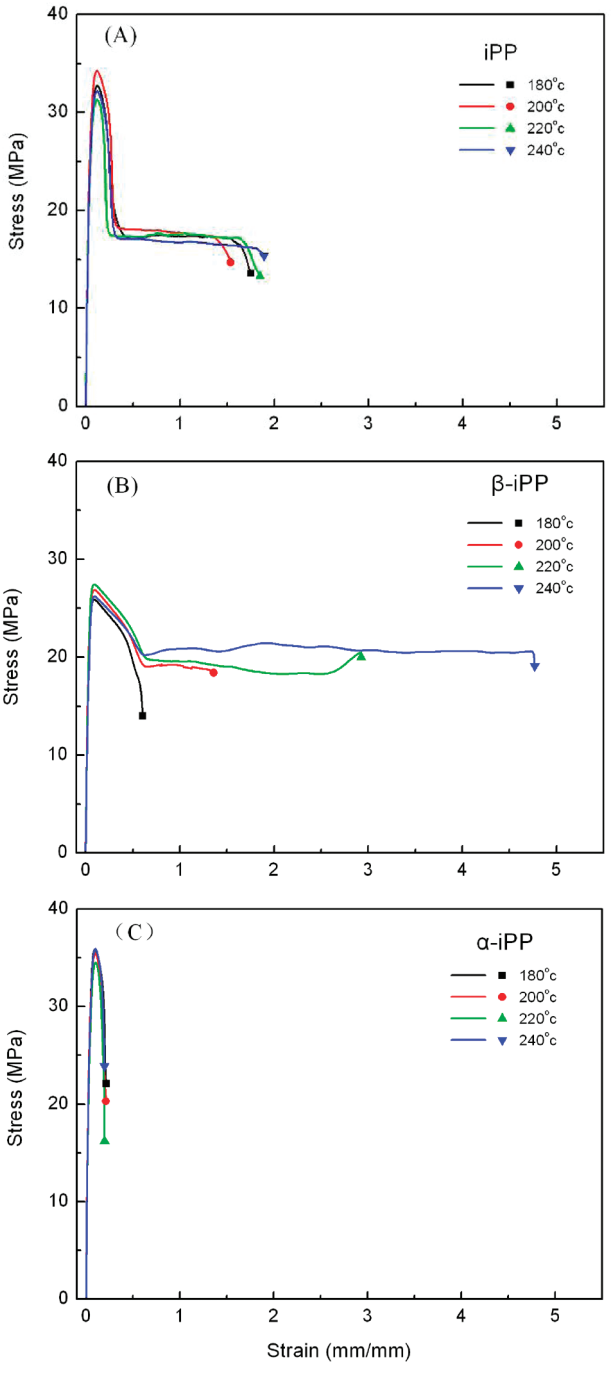

Figure 1. Stress−strain curves for pure iPP, α-nucleated iPP, and β-nucleated iPP samples prepared upon different T_f values: (A) pure iPP, (B) β-nucleated iPP containing 0.25 wt % WBG, and (C) α-nucleated iPP containing 0.25 wt % DMDBS.

that the elongation at break strongly depends on T_f. The elongation is prominently increased from 60 to 476% with the T_f elevated from 180 to 240 °C. It is well-known that the elongation at break can approximately represent toughness because the area under the stress−strain curve represents the energy to failure. Therefore, the tensile test results indicate that (i) the β-nucleated iPP bar does not always show good toughness and (ii) a higher molten temperature during compression molding can result in a larger strain at break.

It is well-known that the notched izod impact strength can reflect toughness directly. The impact strengths for pure iPP, α-nucleated iPP, and β-nucleated iPP are plotted as a function of T_f, as shown in Figure 2. For both pure iPP and α-nucleated iPP, there is a slight decrease in impact strength with increasing T_f, especially at relative high molten temperatures, such as 220 and 240 °C. Within the whole range of T_f, the impact strength of α-nucleated iPP is lower than that of neat iPP, and this result is in agreement with the tensile test result. The impact strength is improved significantly compared with that of pure iPP bars with additional 0.25 wt % WBG. This indicates that β-nucleating agent is effective for toughening iPP. Meanwhile, the impact strength of β-nucleated iPP has increased with increasing T_f. The increase in impact strength is even more pronounced for the comparison made between pure iPP and β-nucleated iPP; the increase in impact strength for the β-iPP prepared at T_f = 240 °C is 3.7 KJ/m^2, which is much larger than that for the β-iPP prepared at T_f = 180 °C, 2.1 KJ/m^2.

Although both elongation at break and impact strength are suitable for estimating toughness, the results obtained from the above two properties are quite different. For example, the toughness of β-nucleated PP evaluated by stress−strain curve improves by 800% when T_f is increased from 180 to 240 °C, whereas the increase in impact tests is only ~20%. The result of the impact tests shows a much lower increase in toughness compared with that of tensile tests. These differences are widely reported[25,26] and likely caused by a difference in the failure mechanism between tensile test and impact test. The cross-head speed in the tensile test is much lower than that in the impact test. Loading rate must play an important role in the failure mechanism. More systematic and profound studies are needed to elucidate this subject. It is out of the scope of this article. However, an obvious T_f dependence on toughness has already been shown in β-nucleated iPP by both measurement methods. Subsequently, the origin of this phenomenon will be explored in detail by following structural and morphological characterizations.

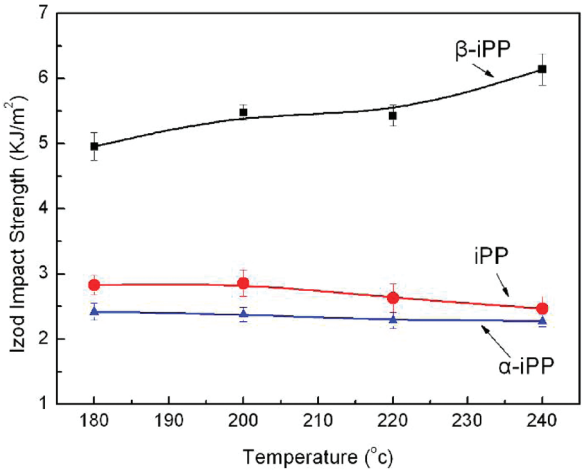

Figure 2. Notched izod impact strength for pure iPP, α-nucleated iPP, and β-nucleated iPP bars as a function of T_f.

3.2. Polymorphic Composition and Crystallinity in the β-Nucleated iPP. It is well-known that the polymorphic composition and overall crystallinity are two important issues for determining the macroscopic toughness of β-nucleated iPP. The effect of T_f on the polymorphic composition and crystallinity should be elucidated clearly. Wide-angle X-ray diffraction (WAXD) was adopted to obtain information about the crystalline type, relative crystallinity of β-phase, and overall crystallinity. The WAXD spectra for iPP containing 0.25 wt % WBG compression-molded under various T_f values are shown in Figure 3. Sharp peaks can be observed at 2θ = 16.1°, which is the characteristic peak of the (300) plane of the β-form. This result clearly indicates that the addition of WBG can largely induce the formation of β-crystal within the T_f range investigated. Meanwhile, the characteristic peaks of the monoclinic α-form are extremely weak. Quantitative estimations of total crystallinity (X_c) and relative fraction of β-form (K_β) have been done according to the methods mentioned in the Experimental Section, and the values are listed in Table 1. For both X_c and K_β, there is no apparent difference between various T_f values, and the values are approximately 57 and 90% for X_c and K_β, respectively. Moreover, some similar results have been achieved through calorimetric analysis (DSC), which can be seen in the Supporting Information. Therefore, the overall crystallinity and proportion of α-form versus β-form in the β-nucleated iPP bar are kept constant for various T_f values.

3.3. Supermolecular Structure of β-Nucleated iPP. Because almost the same polymorphic composition and crystallinity between different T_f values were obtained in β-nucleated iPP, the increase in toughness can only be ascribed to the change of crystal morphology caused by difference in T_f. Therefore, the effect of final molten temperature on the supermolecular structure of β-form iPP has been investigated in detail through SEM and PLM.

The supermolecular structures of β-iPP in the compression-molded bars were studied by SEM. Three types of β-iPP crystalline morphology were indicated for different final

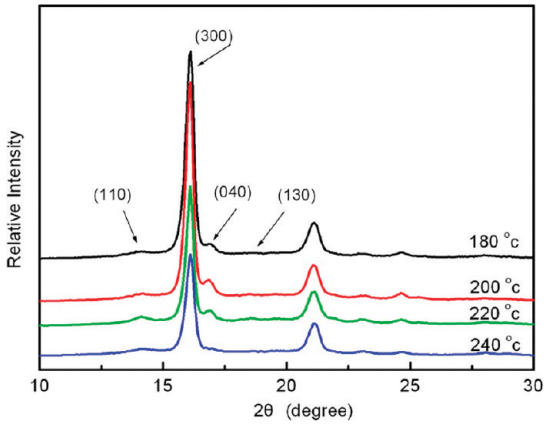

Figure 3. WAXD spectra for β-nucleated iPP samples compression-molded under various T_f values.

Table 1. Values of K_β Obtained by WAXD for β-iPP Samples Prepared upon Various T_f Values

	T_f = 180 °C	T_f = 200 °C	T_f = 220 °C	T_f = 240 °C
X_c (%)	58	57	57	57
K_β (%)	91	89	88	91

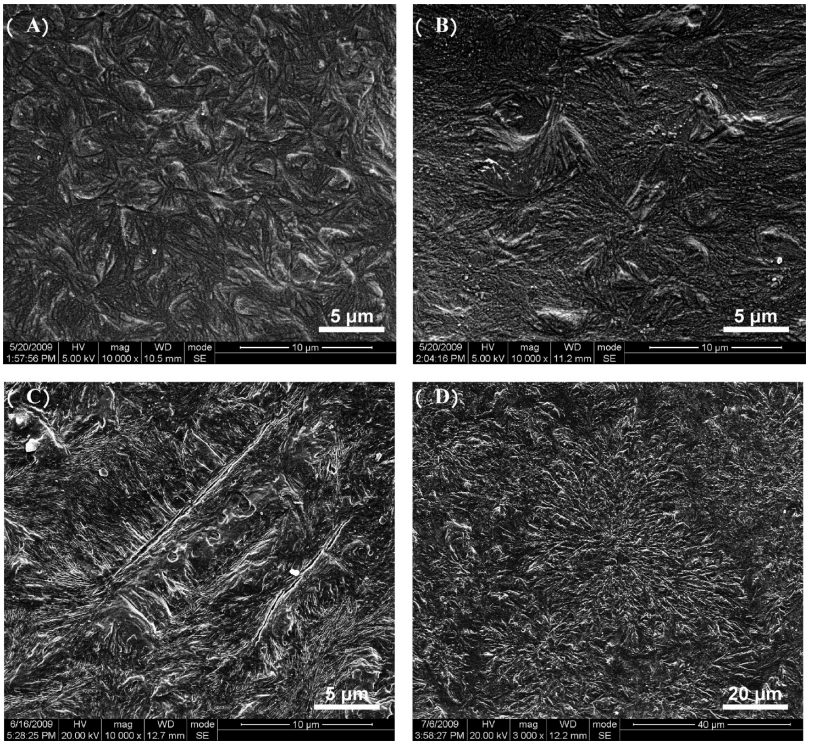

Figure 4. SEM photographs for the supermolecular structures of β-nucleated iPP bars compression-molded under various T_f values: (A) T_f = 180 °C, (B) T_f = 200 °C, (C) T_f = 220 °C, and (D) T_f = 240 °C.

molten temperatures, such as β-spherulites for low T_f values of 180 and 200 °C, β-transcrystalline entities for intermediate T_f of 220 °C, and "flower"-like agglomerates for high T_f of 240 °C. The refined features of β-nucleated crystalline morphologies generated from different T_f values are described as the following on the basis of the SEM micrographs shown in Figure 4. The micrograph of Figure 4a refers to the morphology of the bunching β-spherulite obtained at T_f = 180 °C. The sizes of these spherulites are small, the size distribution is nonuniform, and lamellar arrangement in these spherulites shows irregular distortion. More uniform bunching β-spherulites in the molded bar prepared at T_f = 200 °C are observed in Figure 4b. The spherulite size at this T_f is larger than that at T_f = 180 °C. For the molded bar prepared at T_f = 220 °C (Figure 4c), it appears to be a leaflike transcrystalline structure with ordering lamellae arrangement perpendicular to the needlelike entity of WBG. An entirely different crystalline morphology has been generated in the molded bar prepared at T_f = 240 °C in which the oval-like lamellae was circularly arranged and the "flower"-like agglomerates were observed, as shown in Figure 4d.

To ascertain the formation mechanisms of various β-crystalline morphologies, the crystallization processes started from different T_f values have been investigated by in situ PLM observations. Some typical PLM photographs are presented in Figure 5. For each T_f, three photographs were acquired at the beginning, medium, and end stages of the cooling process. Because of the high β-selectivity and nucleating efficiency of WBG on iPP crystallization, the photograph is almost occupied by the β-crystal of iPP, which shows highly birefringent character and will be completely molten at about 155 °C.[27] However, the solubility of WBG in iPP varies with different T_f, and the self-organization and recrystallization of molten WBG from iPP matrix behaves differently when the cooling process begins from different T_f values. For T_f = 180 °C, the melt of WBG is incomplete, and the melt viscosity is relatively high. The self-organization of tiny granules of WBG does not occur. Therefore, WBG exists as a fashion of dot nucleus. Subsequent crystallization of iPP on such dot nuclei results in spherulitic morphology, as shown in Figure 5a. Once T_f is ascended to 200 °C, the solubility of WBG is promoted modestly, and the viscosity is decreased. The low-level self-organization of WBG substance has taken place before iPP crystallization because nuclei with low anisotropic aspect can be detected in the photographs in the beginning and medium stages. These nuclei with low anisotropy also induce spherulite growth. Under this condition, less aggregation of WBG granules occurs, and the nuclei density is lower than the case of 180 °C. Therefore, the size of spherulit at T_f = 200 °C is larger than that at T_f = 180 °C. In the case of further increasing T_f to 220 °C, the solubility of WBG becomes better, WBG substance easily self-assembles into highly anisotropic entity, needlelike nuclei, as shown in the photograph in the begin stage of Figure 5c. Certainly, needlelike nuclei of WBG cause β-transcrystalline superstructure, as observed in the end stage of Figure 5c. Finally, at T_f = 240 °C, WBG substance is completely molten and high level of self-organization occurs for WBG during recrystallization process. As shown in the photograph in the medium stage of Figure 5d, WBG substance self-assembles into a more complicated framework-like dendrite, which nucleates the subsequent iPP crystallization into the "flower"-like agglomerate of β-crystal. To understand the formation processes precisely, the schematic representations of β-crystal superstructure growth upon different T_f values are plotted in Figure 6. According to Figure 5, three types of precursor for β-crystal are generated through self-assembling WBG substance upon different T_f values, including dot nuclei for 180 and 200 °C, needlelike nuclei for 220 °C, and dendritic framework for 240 °C, whereas these precursors of WBG crystal subsequently nucleate iPP into β-spherulites, β-transcrystalline entities, and "flower"-like agglomerate of β-crystallites, respectively. Therefore, the reason that

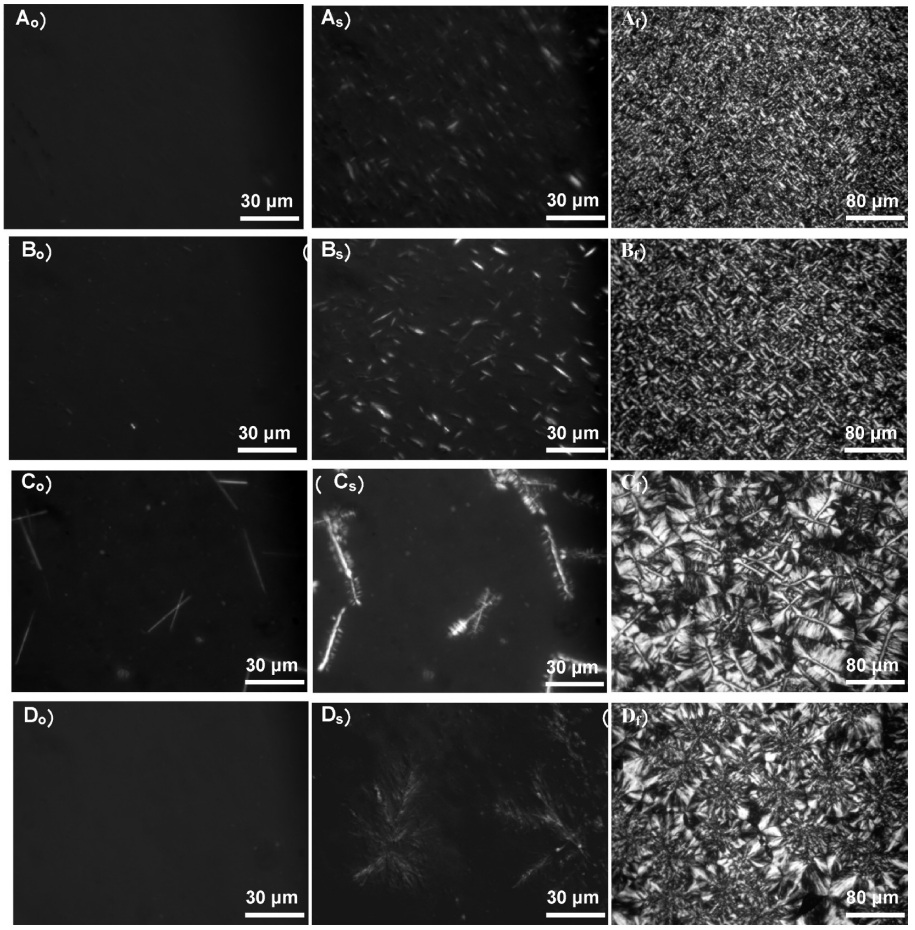

Figure 5. Some typical PLM photographs represent the crystallization of β-nucleated iPP samples heated at different T_f values. (A,B,C,D) T_f = 180, 200, 220, and 240 °C, respectively. The subscripts "o", "s", and "f" represent the stages of original morphology at various T_f values, starting crystal morphology, and final morphology, respectively.

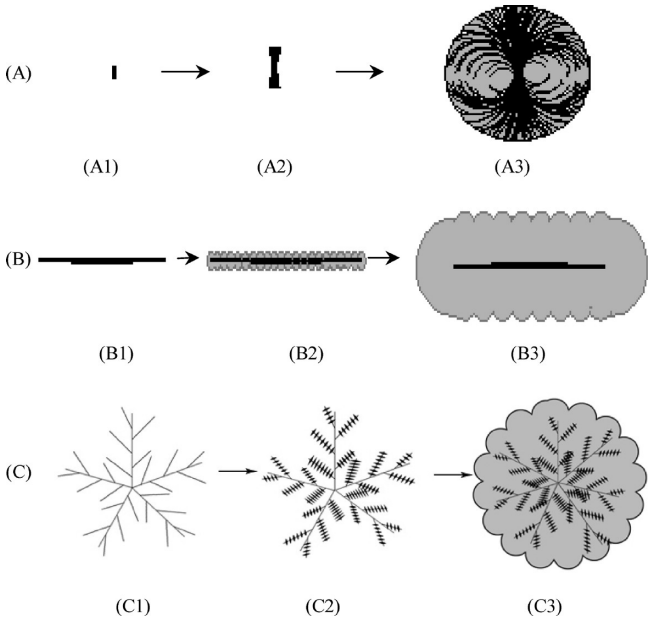

Figure 6. Schematic crystallization processes of β-nucleated iPP cooling from different T_f values: (A) β-spherulite (T_f = 180 and 200 °C), (B) β-transcrystalline entity (T_f = 220 °C), and (C) "flower"-like agglomerate of β-crystallites (T_f = 240 °C).

β-crystalline morphology is strongly dependent on T_f is mainly attributed to the differences in the solubility and self-organization behavior of WBG between different T_f values.

3.4. Role of β-Nucleated Crystalline Morphology on Tuning of Toughness. From the structure−property relation perspective, the macroscopic toughness of semicrystalline polymer (such as iPP) is strongly influenced by various structural and morphological issues, including crystal type, crystalline morphology, crystallinity, and polymorphic composition. Because of the excellent β-selectivity and nucleating efficiency of the rare earth nucleator, the crystal types, overall crystallinity, and β-form content in the compression-molded bar are almost the same between different final molten temperatures. The effects of these crystalline issues on toughness are limited. Therefore, the continuous increase in toughness with elevation of T_f could only be attributed to the variation of β-crystalline morphology with elevation of T_f. In the other words, β-crystalline morphology should play a dominant role in the toughening of β-nucleated iPP. Another evidence to support this conclusion is that in the compression-molded bars of α-nucleated iPP, the crystalline morphologies are identical for various T_f values, which show as numerous tiny spherulites. (See the Supporting Information.) The nucleating mode in α-nucleated iPP is similar to that in the β-nucleated iPP, which is facilitated by the additive nucleator. The toughness of α-nucleated iPP cannot be promoted by increasing T_f because of the fact that there is no obvious difference in α-crystalline morphology between different T_f values. Subsequently, it is necessary to profoundly elucidate the mechanism of β-crystalline

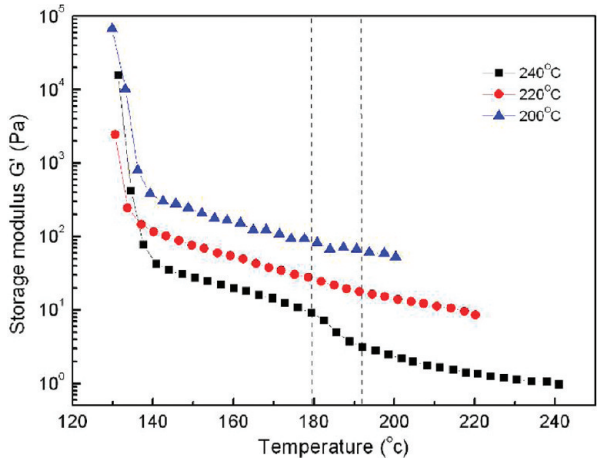

Figure 7. Storage modulus as a function of temperature for β-nucleated iPP samples cooling from different T_f values.

morphology tuning toughness on the basis of the data achieved in this study.

As mentioned above, the origin of β-crystalline morphology strongly depended on T_f. It is mainly due to the differences in the solubility and self-organization behavior of WBG at different T_f values. The dissolubility of WBG is better under a higher molten temperature, and the self-organization capability of WBG is caused by its special chemical structure that may result in the formation of intermolecular hydrogen bonds.[28] It can be envisaged that the melt-cooling process from a higher molten temperature can result in a better solubility for WBG, lower melt viscosity, and longer processing time, which all benefit the occurrence of self-organization of WBG substance during its recrystallization. The self-organization level increases gradually with elevating T_f and can be summarized as the following: no self-assembling takes place and WBG substance exists as individual dot nuclei at T_f = 180 °C, subtle 1D self-organization results in crystalline precursors with low anisotropy at T_f = 200 °C, substantial 1D self-organization leads to needlelike nuclei with high anisotropy at T_f = 220 °C, and WBG substance self-assembles into radial multidirectional framework, dendrite, at T_f = 240 °C. The connection between β-nuclei can be improved by varying crystalline morphology; in particular, for the dendritic entities formed upon T_f at 240 °C, the connectivity between dendrites is strong, and the melt system could contain a network formed by β-nucleating agent. The formation of β-nucleating agent network in the melt cooled from high T_f can be verified indirectly by rheological measurement. As shown in Figure 7, log G′ is plotted as a function of cooling temperature. Whereas the melt of iPP containing 0.25 wt % WBG is cooled from T_f of 200 and 220 °C, log G′ is linearly increased with decreasing temperature before the matrix crystallization. This corresponds to a typical Arrhenius behavior. While the melt is cooled from T_f of 240 °C, an additional reinforcement in log G′ appears within the range from 190 to 180 °C, which implies that during the cooling process the well molten nucleators recrystallize into network structure. Therefore, the viscoelastic property of melt is enhanced, and the whole melt behaves as a physical gelation state. Obviously, the nucleating agent network is easily established during the recrystallization of molten WBG in PP melt cooled from a high T_f. The crystalline system of β-nucleated PP built basically on such nucleating agent network possesses good integrity and synergic effect of numerous β-crystals for resisting deformation and destruction, which is shown as an increase in tensile elongation and impact toughness. Therefore, the toughening effect observed in this study is attributed to the significantly increased connectivity between intercrystallites through the formation of special β-crystalline morphology.

4. Conclusions

A new rare earth nucleating agent, WBG, with high β-selectivity and efficiency has been adopted to prepare compression-molded bar of iPP with constant content of β-form and crystallinity, but variable crystal morphology is obtained by altering the final molten temperature. After the addition of 0.25 wt % WBG to iPP, the toughness is prominently improved. Three types of β-crystalline morphologies, β-spherulite, β-transcrystalline entity, and "flower"-like agglomerate of β-crystallites, are sequentially generated in the molded bars with increasing T_f. The β-nucleated crystalline morphology formed from a higher T_f is more favorable for toughening. A toughening mechanism involving the formation of nucleating agent network during the recrystallization of molten WBG substance is proposed to interpret this phenomenon. It has been demonstrated that the connection between crystallites might mainly determine the toughness of iPP instead of the β-crystal form content.

Acknowledgment. We would like to express our sincere thanks to the National Natural Science Foundation of China for Financial Support (50533050, 20874064, 50873063).

Supporting Information Available: SEM micrograph of raw WBG substance, calorimetric curves of β-nucleated PP, PLM photographs of crystalline morphology of α-nucleated PP, and crystalline properties measured from DSC. This material is available free of charge via the Internet at http://pubs.acs.org.

References and Notes

(1) Padden, F. J.; Keith, H. D. *J. Appl. Phys.* **1959**, *30*, 1479.
(2) Morrow, D. R.; Newman, B. A. *J. Appl. Phys.* **1968**, *39*, 4944.
(3) Meille, S. V.; Bruckner, S.; Porzio, W. *Macromolecules* **1990**, *23*, 4114.
(4) Lotz, B.; Graff, S.; Straupe, C.; Wittmann, J. C. *Polymer* **1991**, *32*, 2902.
(5) Turner-Jones, A.; Aizlewood, J.; Beckett, D. *Macromol. Chem. Phys.* **1964**, *75*, 34.
(6) Fujiwara, Y. *Colloid Polym. Sci.* **1975**, *253*, 273.
(7) Dragaun, H.; Hubeny, H.; Muschik, H. *J. Polym. Sci., Part B: Polym. Phys.* **1977**, *15*, 1779.
(8) Byelov, D.; Panine, P.; Remerie, K.; Biemond, E.; Alfonso, G. C. *Polymer* **2008**, *49*, 3076.
(9) Varga, J.; Karger-Kocsis, J. *Polymer* **1995**, *36*, 4877.
(10) Ellis, G.; Gomez, M. A.; Marco, C. *J. Macromol. Sci. Phys.* **2004**, *43*, 191.
(11) Garbarczyk, J.; Paukszta, D. *Polymer* **1981**, *22*, 562.
(12) Li, J. X.; Cheung, W. L. *Polymer* **1999**, *40*, 2085.
(13) Zhou, J.; Liu, G.; Yan, S.; Dong, J.; Li, L.; Chan, C. *Polymer* **2005**, *46*, 4077.
(14) Stocker, W.; Schumacher, M.; Graff, S.; Thierry, A.; Wittmann, J. C.; Lotz, B. *Macromolecules* **1998**, *31*, 807.
(15) Grigoryeva, O. P.; Karger-Kocsis *J. Eur. Polym.* **2000**, *36*, 1419.
(16) Huy, T. A.; Adhikari, R.; Lupke, T.; Henning, S.; Michler, G. H. *J. Polym. Sci., Polym. Phys. Ed.* **2004**, *42*, 4478.
(17) Lezak, E.; Bartczak, Z.; Galeski, A. *Polymer* **2006**, *47*, 8562.
(18) Li, J. X.; Cheung, W. L.; Chan, C. M. *Polymer* **1999**, *40*, 2089.
(19) Chu, F.; Yamaoka, T.; Kimura, Y. *Polymer* **1995**, *36*, 2523.
(20) Varga, J.; Menyhárd, A. *Macromolecules* **2007**, *40*, 2422.
(21) Xiao, W. C.; Wu, P. Y.; Feng, J. C. *J. Appl. Polym. Sci.* **2009**, *111*, 1076.
(22) Xiao, W. C.; Wu, P. Y.; Feng, J. C.; Yao, R. Y. *J. Appl. Polym. Sci.* **2008**, *108*, 3370.

(23) Huo, H.; Jiang, S. J.; An, L. J.; Feng, J. C. *Macromolecules* **2004**, *37*, 2478.
(24) Olley, R. H.; Bassett, D. C. *Polymer* **1982**, *3*, 1707.
(25) Kotek, J.; Raab, M.; Baldrian, J.; Grellmann, W. *J. Appl. Polym. Sci.* **2002**, *85*, 1174.
(26) Tjong, S. C.; Shen, J. S.; Li, R. K. Y. *Polym. Eng. Sci.* **1996**, *36*, 100.
(27) Varga, J. *J. Macromol. Sci. Phys.* **2002**, *B41*, 1121.
(28) Behrendt, N.; Mohmeyer, N.; Hillenbrand, J.; Klaiber, M.; Zhang, X.; Sessler, G. M. *J. Appl. Polym. Sci.* **2006**, *99*, 650.